Magnetic relaxation in $Tl_2Ba_2CaCu_2O_8$ single crystals by SQUID magnetometer and micro-Hall sensor

P. Chowdhury, Heon-Jung Kim, W. N. Kang, Dong-Jin Zang, and Sung-Ik Lee*
National Creative Research Initiative Center for Superconductivity and Department of Physics, Pohang University of Science and Technology, Pohang 790-784, Republic of Korea

D. H. Kim
Department of Physics, Yeungnam University, Kyungsan 712-749, Republic of Korea
(Received 18 March 2003; revised manuscript received 16 June 2003; published 8 October 2003)

Measurements of the isothermal magnetization hysteresis loops $M(H)$ and the magnetic relaxation for a $Tl_2Ba_2CaCu_2O_8$ single crystal were carried out by using a superconducting quantum interference device magnetometer and a micro-Hall sensor. In the temperature window from 30 to 60 K, the measurements for $M(H)$ show a second anomalous peak at a field H_{sp} and an onset field of H_{on}. From these relaxation data measured by two different techniques, the activation barrier U_0 and the creep exponent μ were separately calculated as functions of H based on the weak collective pinning theory. The variation of the normalized creep rate, $S=(|d \ln M/d \ln t|)$, with H is also presented. The results at $T=35$ K indicate that at a characteristic field H^* lying between H_{on} and H_{sp}, a minimum is observed in $S(H)$ whereas a maximum is observed in $U_0(H)$. These analyses also show that below H^*, the creep phenomenon is controlled by an elastic process. However, above H_{sp} a negative power law, $U_0(H) \propto H^{\nu}$ with $\nu \sim -0.9$, is observed suggesting the existence of plastic creep. At a low temperature of $T=20$ K, where no second peak is observed, both $S(H)$ and $U_0(H)$ behave differently. A comparative study of the different creep parameters obtained from the two different measurement techniques is also discussed.

DOI: 10.1103/PhysRevB.68.134413 PACS number(s): 74.25.Qt, 74.72.Jt, 74.25.Ha

The study of the vortex phase diagram in high-temperature superconductors (HTSC) is an important issue not only for technical applications but also for basic research because various vortex phases have been predicted theoretically[1] and observed experimentally. The most extensive studies on vortex matter have been carried out on $YBa_2Cu_3O_{6+y}$ (YBCO) and $Bi_2Sr_2CaCu_2O_{8+y}$ (BSCCO) single crystals,[2–6] and the interesting feature was the appearance of a second magnetization peak (SMP) starting at a field of H_{on} far above the first thermodynamical critical field H_{c1}. Several explanations have been suggested for the origin of this peak: matching between the vortex lattice and crystal defects,[2] surface-barrier effects,[3,4] a dimensional crossover in the vortex dynamics,[7,8] a weak first-order vortex lattice melting,[5] and layer decoupling.[9]

Theoretically, different vortex phases are predicted when different energies, such as the elastic, the pinning, and the thermal energies are balanced.[10,11] The shape of vortex melting curve, which is characterized by a first-order thermodynamic transition, is determined by a competition between the elastic and the thermal energies[12] whereas an entangled line, which manifests itself as the onset of a second magnetization peak at a field of H_{on} in the $M(H)$ hysteresis loops, can be described by a competition between the pinning and the elastic energies.[13] The magnetic relaxation studies are very useful tools for understanding the precise characteristics of different phases and the phase boundaries across the SMP and give important information on the vortex activation energy and the creep characteristics in HTSC. Recently, magnetic relaxation studies were carried out on YBCO,[14,15] pure BSCCO,[16–18] and Pb-doped BSCCO[19] single crystals by several groups. Though the creep phenomenon was well explained based on the weak collective pinning theory (WCPT) for fields below the second peak field H_{sp}, above it the existence of the dislocation-mediated plastic creep was confirmed, and the crossover from elastic to plastic creep was shown to be the origin of the second peak.[14–17,19]

Studies on the $Tl_2Ba_2CaCu_2O_8$ (TBCCO) system in single-crystalline form have been hampered due to the toxicity of Tl_2O_3 and the high vapor pressure of Tl at the synthesis temperature. Recently, our reports on the irreversible magnetization, the reversible magnetization, the remanent magnetization, and the transport properties[20–23] of this material revealed that these crystals had good quality and the physical properties were comparable with those observed in other high-T_c materials. The field-dependent magnetic relaxation in this compound has not been well studied so far in single-crystalline form. In a report, Wen *et al.*[24] claimed to have observed two regions of vortex dynamics while analyzing their relaxation data for TBCCO thin films; three-dimensional (3D) vortex motion occurred via an elastic creep in the low-field region while plastic creep occurred at higher fields following a 3D to 2D transition at a field of 0.7 T. It should be mentioned that in thin films, the grain boundary itself can act as a strong pinning center which may control the intrinsic properties of the material. Thus, in this report, we discuss the evolution of the creep characteristics in the H-T plane for TBCCO single crystals at different temperatures by using relaxation measurements with both a superconducting quantum interference device (SQUID) magnetometer and a Hall sensor.

Single crystals of $Tl_2Ba_2CaCu_2O_8$ were grown from a stoichiometric mixture of Tl_2O_3 and a precursor

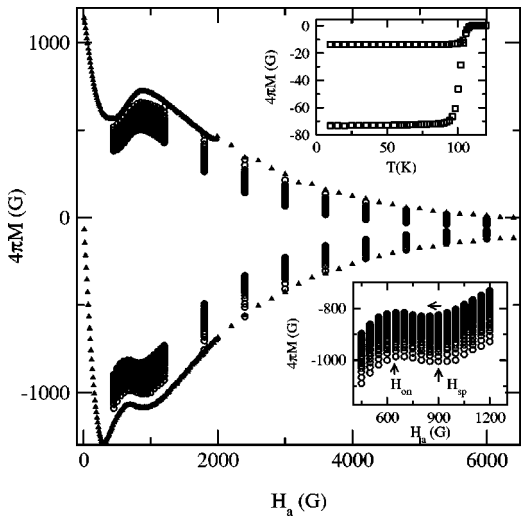

FIG. 1. Field-dependent magnetization and magnetic relaxation measured by using a SQUID magnetometer at a temperature of $T=35$ K. The upper inset shows $M(T)$ measured at field of $H=10$ G. The lower inset shows an enlarged view of the magnetic relaxation in the vicinity of the second peak field H_{sp}.

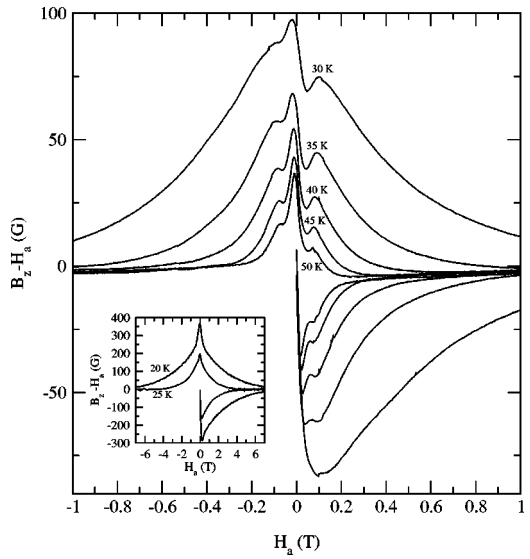

FIG. 2. Field-dependent local magnetization measured by using a Hall sensor and at temperatures in the range from 30 to 50 K. The inset shows the same data for temperatures of 20 K and 25 K.

$Ba_2CaCu_2O_x$. Details of the growth procedure are reported elsewhere.[20,21] A structural characterization of these crystals, which was obtained by using x-ray diffraction, is also presented in Ref. 20. Several crystals, with average dimensions of $1\times1\times0.2$ mm^3, were characterized by using the magnetization measurements. Extensive relaxation measurements were carried out on a sample with $T_c\sim105$ K. The transition width was around 5 K, as determined from the M-T measurement at a field of 10 G, as shown in the inset (upper right corner) of Fig. 1.

At first, the magnetic hysteresis loop $M(H)$ and the relaxation measurements were performed at different temperatures by using a SQUID magnetometer (Quantum Design) with the external magnetic field applied parallel to the c axis. A typical $M(H)$ loop and the magnetic relaxations measurements at a temperature of 35 K are shown in Fig. 1. After cooling down the sample in zero field to the set temperature, the whole $M(H)$ loop was recorded with increasing fields in steps with the most possible rapid way in our technique. For the relaxation measurement we repeated the same loop, but at each measurement field we recorded the magnetization as a function of time for 4000 sec. For fields below 1200 G, the step in the field of 50 G after the end of each relaxation process produces an initial magnetization which lies within 5–8 % of the value of the original $M(H)$ loop corresponding to that field. These small deviations are due to the fact that this step is smaller than the first field for full flux penetration, but we will see later that the above intermittent field increase procedure does not affect the determination of correct values of the physical parameters. To confirm that, we have also performed a relaxation measurement as a reference at a field of 850 G. During this measurement, the sample was cooled down at 35 K in zero field and then after ramping the field to 850 G, the magnetization data was recorded for 10 000 sec.

At this temperature (35 K), the anomalous SMP is observed at $H_{sp}=950$ G whereas the onset field is observed at $H_{on}=650$ G as shown in the inset (lower right corner) of Fig. 1. For this material, a systematic study of $M(H)$ measured by using a SQUID magnetometer for a wide temperature window are reported in Ref. 20; the temperature dependences of both H_{sp} and H_{on} are also presented. However, these global magnetization measurements are averages over regions of different local inductions across the sample; thus, because of the sample's shape, square or rectangular blocks, edge effects cannot be neglected. For that reason, as discussed in the next paragraph, local induction as well as magnetic relaxation measurements were performed on this sample by using a Hall sensor.

For the local measurements, an InSb Hall sensor with a sensing area of $100\times100\ \mu$m^2 and a resolution of 0.46 μV/G was used. The sensor was placed at the center of the crystal. The magnetic measurements were performed by using a Maglab2000 (Oxford) system, where magnetic fields up to 7 T could be applied by using a superconducting magnet and a temperature accuracy of 5 mK could be achieved. The local magnetization was defined as the difference between the field measured by using the Hall sensor, B_z, and the applied field H_a. The local $M(H)$ loops measured at different temperatures are shown in Fig. 2. It is clear from this figure that the shapes of the $M(H)$ loops measured at different temperatures are similar to that observed in the SQUID measurements. For the local measurements at $T=35$ K, the onset field H_{on} and the second peak field H_{sp} are observed at 650 ± 10 G and 950 ± 10 G, respectively. These values are similar to those obtained from the global magnetization measurements.[25,26]

Figures 3(a) and 3(b) present the behavior of the irreversible magnetization M_{irr} for flux entry as a function of ln(t) at $T=35$ K and in the vicinity of second peak field H_{sp} as measured by using a SQUID magnetometer and a Hall sensor, respectively. In the inset of Fig. 3(a), M_{irr} for flux entry measured by using a SQUID magnetometer as a reference,

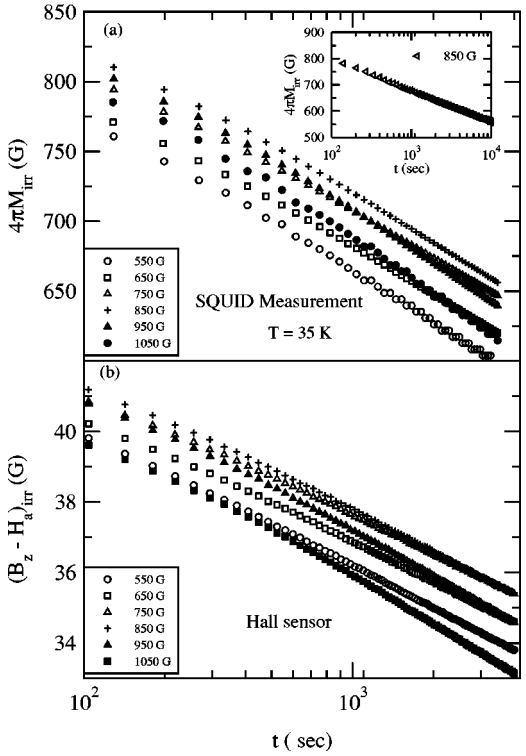

FIG. 3. M_{irr} for flux entry at $T=35$ K as a function of $\ln(t)$ in the vicinity of the second peak field H_{sp} measured (a) by using a SQUID magnetometer and (b) by using a Hall sensor. The upper inset shows the same measured by using a SQUID magnetometer as a reference for the time window 100–10 000 sec at a field of 850 G. Please see the text for details.

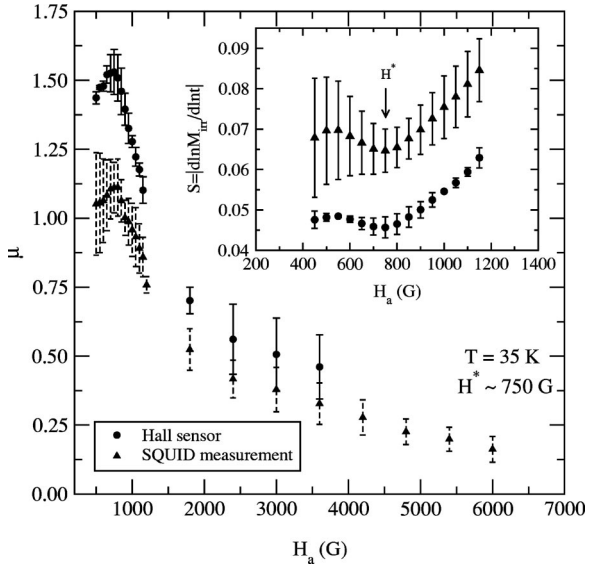

FIG. 4. Variation of creep exponent $\mu(H)$ at $T=35$ K measured by using a SQUID magnetometer and a Hall sensor. The normalized creep rates S obtained from these two different techniques are shown in the inset.

for the time window 100–10 000 s at a field of 850 G, is shown. At the initial time, i.e., $t=t_1$, the nonrelaxing reversible magnetization of the sample, $M_{rev}=[M_+(t_1)+M_-(t_1)]/2$, was calculated, and then the irreversible magnetizations $M_{irr}(t)=M_{\pm}(t)\mp M_{rev}$ were calculated for both flux entry and flux exit. Here, $M_+(t)$ and $M_-(t)$ are the measured magnetizations for flux entry and flux exit, respectively. Both the figures show a nonlogarithmic behavior of $M_{irr}(t)$, particularly at longer time t, which implies that the Anderson-Kim model[27] cannot be applied to analyze these relaxation data.

For the physical interpretation of the relaxation behavior, we start with the prediction of the WCPT, where the activation energy $U(j)$ for $j \ll j_c$ is given by[1,28,29]

$$U(j)=U_0(H)(j_c/j)^{\mu}, \tag{1}$$

where $U_0(H)$ is the collective pinning barrier, which increases with the applied magnetic field, and j_c is the critical current density. The values of the exponent μ identify the various collective creep regions and depend on the magnitudes of the field and the current. For a three-dimensional vortex system, $\mu=1/7$ corresponds to the single vortex creep region at low fields and high currents, $\mu=3/2$ to the small bundle creep region at intermediate currents and fields, $\mu=1$ to the creep of intermediate vortex bundle creep region, and $\mu=7/9$ to the large vortex bundle creep region at low currents and high fields.

Based on this theory, $M_{irr}(t) \propto j(t)$ can be described by the relation

$$M_{irr}(t)=M_{irr}(0)\left[\frac{\mu k_B T}{U_0}\ln(t/t_0)\right]^{-1/\mu}, \tag{2}$$

where t_0 is some attempt time. It should be mentioned that Eq. (2) is valid only for $j \ll j_c$. To satisfy the above condition, we fitted this equation to the experimentally observed $M_{irr}(t)$ curve for the time window 400–4000 sec, and we calculated both U_0 and μ for different fields for both flux exit and flux entry. Here, the value of t_0 was fixed to 10^{-3} sec as reported for BSCCO single crystals.[30] The normalized creep rate S was calculated by using the relation $S=|d\ln M_{irr}/d\ln t|$ for all the described fields and for both flux exit and entry. While plotting these parameters, we took an average of the data obtained for flux exit and flux entry for each field; we show the deviations as error bars. It is observed that the values of all the parameters obtained from the data measured by using SQUID magnetometer were found to lie systematically above the average for flux exit and below for flux entry. But this is not true for the case of Hall sensor measurements as the deviations were found to be very small in comparison to SQUID measurements.

The magnetic-field dependence of the normalized creep rate S measured by using two different techniques at $T=35$ K and in the vicinity of the second magnetization peak field H_{sp} is shown in the inset of Fig. 4. At higher fields, S becomes difficult to calculate as $\ln(M_{irr})$ is no longer linear in $\ln(t)$, particularly at longer times. It is clear from this figure that the local creep rate is lower than the rate obtained from the global magnetization measurements. It is obvious

that, as for the global measurements, S is an average of different local creep values. However, S measured by the two different methods show similar features. At low fields ($\leqslant 550$ G) S starts to increase, and reaches a maximum. With further increasing fields, it starts to decrease and goes to a minimum; then, it increases almost linearly with the applied field. The minimum value occurs at $H^* = 750 \pm 10$ G. With careful investigation, we observed that H^* is located at the point where dM/dH (obtained from the M-H loop) is minimum and lies between H_{on} and H_{sp}. This minimum in S was also observed in both YBCO (Ref. 13) and $La_{2-x}Sr_xCuO_4$ (LSCO) (Ref. 31) single crystals at $H = H_k$, where H_k lies between H_{on} and H_{sp}. The important point is that the decrease of S indicates an enhancement in the effectiveness of pinning. The error bars for the global magnetization measurements are much higher than those for the local measurements. This might be due to the edge effects during flux exit and entry. The global value of $S \sim 0.75 \pm 0.05$ was also calculated from the reference data and found to lie within the error bar obtained from the global measurement using the intermittent field increase procedure.

The variation of μ with H, obtained from both local and global magnetization measurements at $T = 35$ K, is shown in Fig. 4. At this temperature, the global $\mu = 0.92 \pm 0.05$ was also calculated from the reference measurement. As observed for S, it was also found that this μ value lies within the error bar, obtained from the original measurements. This implies that our original procedure will not introduce large error factors in calculating the parameters. The interesting feature observed in Fig. 4 is that the average magnitudes of μ obtained from the local measurements are higher than those from the global measurements, but the shapes of the curves are very similar. This figure also shows that the local μ value starts to increase for fields up to H^*, then, with further increase in the fields, it drops sharply. A comparison of the magnitude of the local μ value with the theoretically predicted values implies the existence of a small bundle creep region at the center of the sample for fields below H^*. However, in this field region, the change in the μ value is not sufficient to quantify any crossover in the creep mechanism, i.e., from intermediate bundle creep region to a small bundle creep region, as observed in YBCO and Pb-doped BSCCO single crystals.[14,19] The global magnetization measurements average different local creep values across the sample, so the average μ calculated from these data, while comparing with local μ value, indicates the existence of a different creep mechanism as one moves far from the center of the sample. This behavior was also reported for BSCCO single crystals based on magnetization studies with a local Hall-probe array.[32] Since the large fluctuation of μ observed in the global measurements below H^* cannot be ruled out as being due to edge effects during flux exit and flux entry, it becomes difficult to identify the actual behavior below this characteristic field. Above H^*, the value of μ measured by two different techniques drops sharply with increasing fields and reaches 0.4–0.2 for fields close to 3500 G. Within the collective pinning theory, this low value of μ indicates a single creep region ($\mu = 1/3$), which is expected for low fields and high values of j.

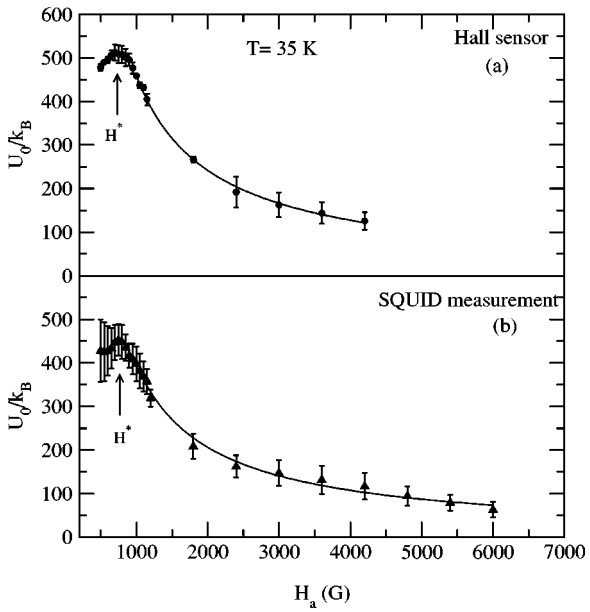

FIG. 5. Variation of $U_0(H)$ at $T = 35$ K measured (a) by using a Hall sensor and (b) by using a SQUID magnetometer. The solid lines are the power-law fits, $U_0(H) \propto H^{-\nu}$, with $\nu = 0.92$ and 0.94 for the local and the global measurements, respectively.

Let us compare our μ value with other reported values. In general, the glassy exponent μ has been determined from the electric field (E)-versus-current(j) or the M-versus-H characteristics by using several formulations based on the assumption of Eq. (1). In TBCCO thin films, the $+$ve μ (0–0.3) region ($B_e < 0.7$ T and $T \leqslant 55$ K) was characterized by 3D vortex states while a wide temperature and field region was found to give $-$ve μ values ($\leqslant -0.3$) characterized by a 2D dislocation-mediated creep. In both YBCO (Refs. 14,33) and LSCO (Ref. 34) single crystals, the μ value first increases with H from 1 to 2 for $H < H_{sp}$ and then decreases continuously towards zero as the field is swept; sometimes negative values are observed at higher fields. A similar result was also reported recently for heavily Pb-doped BSCCO single crystals,[19] where an initial increment of μ up to 2.0 was observed for fields less than H^*, lying between H_{on} to H_{sp}. The value of μ then dropped sharply to 0.2 with further increases in the field. A comparison with other reports[14,19,34] suggests that for fields below H^* or H_{sp}, the creep is controlled by an elastic process, while for fields above these characteristic fields, the sharp decrease in μ suggests the presence of another creep mechanism. This can also be further demonstrated by using the field-dependent pinning potential as discussed below.

Figures 5(a) and 5(b) present the behavior of U_0 as a function of the applied field, obtained by using both Hall sensor and SQUID magnetometer measurements, respectively. It is clear from these figures that the average magnitude for $U_0(H)$ obtained from the local measurements are higher than those from the global measurements, but the shapes are very similar to those observed for $\mu(H)$. These figures also indicate that the local U_0 increases with fields up to H^*, but the large fluctuation of the global values makes it difficult to identify the actual behavior in this field region.

With further increase in the fields (i.e., above H_{sp}), U_0, obtained from both the measurements, follows a negative power-law behavior, $U_0 \propto H^{\nu}$, with ν being -0.92 and -0.94 for local and global magnetization, respectively.

Above H_{sp}, the negative power-law behavior can be compared with other reported experimental results. The values of ν, obtained so far for fields $H > H_{sp}$, lie between ~ -0.5 and -0.7 for YBCO,[14] pure BSCCO,[16] Pb-doped BSCCO,[19] Tl-1212,[17] and $HgBa_2CuO_{4+\delta}$ (HBCO),[35] and are very close to our observed value. In all of the above studies, the negative power law was explained by a dislocation-mediated plastic creep based on the proliferation of dislocations in the entangled vortex structures, as proposed by Abulafia *et al.*[14] For such a plastic creep, the zero current activation energy U_{pl} can be written as[36] $U_{pl} = \epsilon \epsilon a_0$, where $a_0 = (\Phi_0/B)^{1/2}$ is the lattice constant, $\epsilon_0 = \Phi_0^2/4\pi\mu_0\lambda_{ab}^2(T)$, and ϵ is the anisotropy parameter. For a constant temperature, this equation leads to $U_{pl} \propto B^{\nu}$, with $\nu = -1/2$. This negative power implies that for plastic creep, the activation energy U_{pl} always decreases with the field, in contrast with elastic creep where the creep activation energy U_{el} increases with the field.[1]

Based on an analysis of the relaxation data on Pb-doped BSCCO and HBCO single crystals, in the field range $H_{on} < H < H_{sp}$, Sun *et al.*[19] and Pissas *et al.*[35] reported that both creep mechanisms were operating simultaneously and that the dominant creep mechanism was determined by the smaller activation energy between U_{el} and U_{pl}. As the onset of magnetization is believed to result from a competition between the elastic and the pinning energies, for $H > H_{on}$ it might be possible for the elastic energy to become larger than the pinning energy and for vortex interaction with pinning centers to result in an entangled solid where cells of vortex lattice are twisted and dislocations proliferate. This proliferation influences the flux creep mechanism as a dislocation-mediated plastic flux creep in the system, which causes the decrease of the pinning potential with increasing fields. Thus, the competition between U_{pl} and U_{el} results in a maximum for $U_0(H)$ at $H = H^*$. Therefore, below $H < H^*$, as $U_{el} > U_{pl}$, elastic creep controls the flux dynamics, but above H^*, since $U_{pl} > U_{el}$, plastic creep controls the flux dynamics. Therefore, our results indicate that the vortex motion for $H > H_{sp}$ is mainly dominated by dislocation-mediated creep. Similar results were also observed at $T = 45$ K (not shown here).

Based on these relaxation measurements using a Hall sensor and a SQUID magnetometer at $T = 20$ K, we calculated μ as a function of the field H. The results are plotted in Figs. 6(a) and 6(b), respectively; $S(H)$ curves are shown in the insets. The results for $U_0(H)$ are shown in Fig. 7. It should be mentioned that no second peak was observed at this temperature (Fig. 2). From these figures (Figs. 6 and 7), it is clear that the difference in magnitude between the parameters calculated from the local and the global measurements are very small in comparison to those observed at 35 K and those at low fields, i.e., below 4000 G, S and U_0 are almost constant and μ shows a tendency to increase. With further increases in the field, S increases almost linearly, and both μ and U_0 fall rapidly, as observed for $T = 35$ K. However, the field dependence of the activation energy $U_0(H)$ does not follow a negative power law, but shows a logarithmic behavior. In our earlier report on remanent magnetization,[22] we observed that for $T < 27$ K the low-temperature vorticity was characterized by 2D pancake vortices because the collective pinning length L_c was found to be 3 Å $\ll d = 15$ Å, i.e., half of the unit-cell length. It was also mentioned that the thermal depinning temperature $T_{dp}(=30$ K) (Ref. 22) played an important role in changing the creep mechanism for $T > 30$ K,

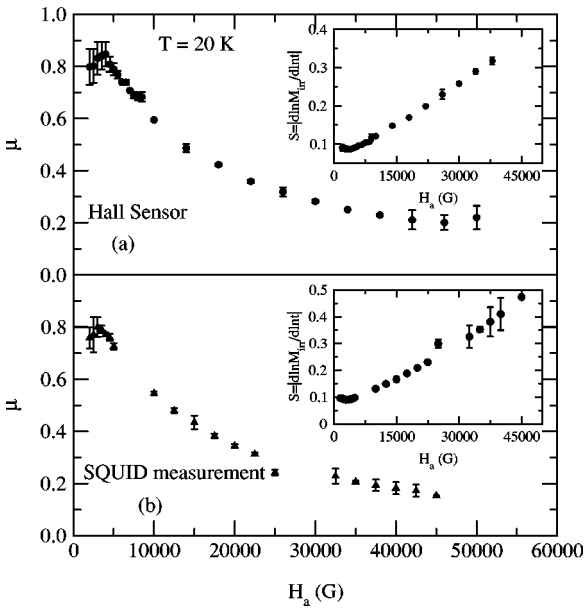

FIG. 6. Variation of the creep exponent $\mu(H)$ at $T = 20$ K measured (a) by using a Hall sensor and (b) by using a SQUID magnetometer. The normalized creep rate S obtained from two different techniques is shown as an inset of this figure.

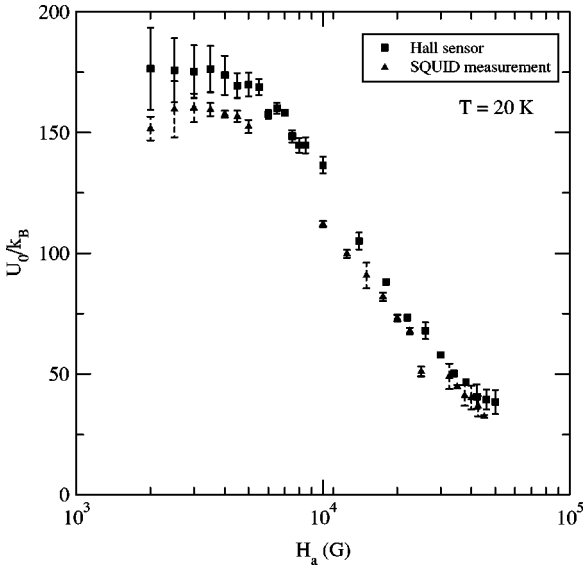

FIG. 7. Variation of $U_0(H)$ at $T = 20$ K measured by using a SQUID magnetometer (triangles) and by using a Hall sensor (squares).

as a sharp fall of the critical current density j_c was observed at this temperature. According to 2D collective pinning theory,[37] the values of μ are 7/4, 13/16, and 1/2 for small bundle, medium bundle, and large bundle vortices, respectively. Our experimental value of $\mu \sim 0.8$ implies the existence of a 2D collective creep (medium bundle) region for fields less than 4000 G. For fields above 4000 G, the sharp decrease of μ to 0.2 and the logarithmic decrease of $U_0(B)$ cannot be explained by this 2D collective pinning theory. This decrease of $U_0(B)$ may signify a crossover from a 2D collective creep to a plastic creep, but origin of the logarithmic behavior is not clear. In contrast to our observation, a recent report on Pb-doped BSCCO single crystals[19] showed the existence of a second peak even at a low temperature of $T=18$ K, but $U_0(H)$ showed an almost constant behavior for fields greater than H_{sp}. It is to be mentioned, however, that Pb-doped BSCCO shows a much lower anisotropy than pure BSCCO and TBCOO. This might indicate that anisotropy plays an important role in influencing the vortex characteristics at low temperatures.

In conclusion, we have performed relaxation measurements on a TBCCO single crystal by using a Hall sensor and a SQUID magnetometer at $T=35$ K and 20 K and for different applied fields. The results show that at $T=35$ K, the magnitudes of the creep parameters S, μ, and U_0 measured by those two different techniques are different, while the functional forms of these parameters with H are very similar. At this temperature, both sets of the results indicate that for fields below a characteristic field H^* lying between H_{on} and H_{sp}, the creep phenomena is controlled by an elastic process. For $H>H_{sp}$, the negative power-law behavior of $U_0(H)$ with an exponent of $\nu \sim -0.9$ indicates the existence of the dislocation-mediated plastic creep. At the low temperature $T=20$ K and at low fields, both $\mu(H)$ and $U_0(H)$ obtained from the two techniques demonstrate the existence of a 2D collective creep. At higher fields, the logarithmic behavior of $U_0(H)$ and the sharp fall of μ might signify a crossover to plastic creep.

This work was supported by the Ministry of Science and Technology of Korea through the Creative Research Initiative Program. This work was partially supported by the National Research Laboratory Program through the Korea Institute of Science and Technology, Evaluation and Planning.

*Corresponding author. Email address: silee@postech.ac.kr.

[1] G. Blatter, M.V. Feigel'man, V.B. Geshkenbein, A.I. Larkin, and V.M. Vinokur, Rev. Mod. Phys. **66**, 1125 (1994).
[2] G. Yang, P. Shang, S.D. Sutton, I.P. Jones, J.S. Abell, and C.E. Gough, Phys. Rev. B **48**, 4054 (1993).
[3] C.D. Dewhurst, D.A. Cardwell, A.M. Campbell, R.A. Doyle, G. Balakrishnan, and D. McK. Paul, Phys. Rev. B **53**, 14 594 (1996).
[4] V.N. Kopylov, A.E. Koshelev, I.F. Schegolev, and T.G. Togonidze, Physica C **170**, 291 (1990).
[5] J. Shi, X.S. Ling, R. Liang, D.A. Bonn, and W.N. Hardy, Phys. Rev. B **60**, R12 593 (1999).
[6] Ming Xu, T.W. Li, D.G. Hinks, G.W. Crabtree, H.M. Jaeger, and Haruyoshi Aoki, Phys. Rev. B **59**, 13 632 (1999).
[7] A.K. Pradhan, S.B. Roy, P. Chaddah, C. Chen, and B.M. Wanklyn, Phys. Rev. B **49**, 12 984 (1994).
[8] F. Zuo, S. Khizroev, G.C. Alexandrakis, and V.N. Kopylov, Phys. Rev. B **52**, R755 (1995).
[9] B. Horovitz, Phys. Rev. B **60**, R9939 (1999).
[10] D. Ertas and D.R. Nelson, Physica C **272**, 79 (1996).
[11] V. Vinokur, B. Khaykovich, E. Zeldov, M. Konczykowski, R.A. Doyle, and P.H. Kes, Physica C **295**, 209 (1998).
[12] N. Avraham, B. Khaykovich, Y. Myasoedov, M. Rappaport, H. Shtrikman, D.E. Feldman, T. Tamegai, P.H. Kes, M. Li, M. Konczykowski, K.V.D. Beek, and E. Zeldov, Nature (London) **411**, 451 (2001).
[13] D. Giller, A. Shaulov, Y. Yeshurun, and J. Giapintzakis, Phys. Rev. B **60**, 106 (1999).
[14] Y. Abulafia, A. Shaulov, Y. Wolfus, R. Prozorov, L. Burlachkov, Y. Yeshurun, D. Majer, E. Zeldov, H. Wuhl, V.B. Geshkenbein, and V.M. Vinokur, Phys. Rev. Lett. **77**, 1596 (1996).
[15] D. Giller, A. Shaulov, R. Prozorov, Y. Abulafia, Y. Wolfus, L. Burlachkov, Y. Yeshurun, E. Zeldov, V.M. Vinokur, J.L. Peng, and R.L. Greene, Phys. Rev. Lett. **79**, 2542 (1997).
[16] L. Miu, E. Cimpoiasu, T. Stein, and C.C. Almasan, Physica C **334**, 1 (2000).
[17] T. Aouaroun, V. Hardy, and Ch. Simon, Physica C **294**, 42 (1998).
[18] D.H. Kim, T.W. Lee, C.W. Lee, D.H. Ha, and S.Y. Shim, Physica C **383**, 23 (2002).
[19] Y.P. Sun, W.H. Song, J.J. Du, and H.C. Ku, Phys. Rev. B **66**, 104520 (2002).
[20] P. Chowdhury, Heon-Jung Kim, In-Sun Jo, and Sung-Ik Lee, Physica C **384**, 411 (2003).
[21] Heon-Jung Kim, P. Chowdhury, In-Sun Jo, and Sung-Ik Lee, Phys. Rev. B **66**, 134508 (2002).
[22] P. Chowdhury, Heon-Jung Kim, In-Sun Jo, and Sung-Ik Lee, Phys. Rev. B **66**, 184509 (2002).
[23] Heon-Jung Kim, P. Chowdhury, W.N. Kang, Dong-Jin Zang, and Sung-Ik Lee, Phys. Rev. B **67**, 144502 (2003).
[24] H.H. Wen, A.F.Th. Hoekstra, R. Griessen, S.L. Yan, L. Fang, and M.S. Si, Phys. Rev. Lett. **79**, 1559 (1997).
[25] M. Konczykowski, L.I. Burlachkov, Y. Yeshurun, and F. Holtzberg, Phys. Rev. B **43**, 13 707 (1991).
[26] Y. Yeshurun, A.P. Malozemoff, and A. Shaulov, Rev. Mod. Phys. **68**, 911 (1996).
[27] P.W. Anderson and Y.B. Kim, Rev. Mod. Phys. **36**, 39 (1964).
[28] A.I. Larkin and Yu.N. Ovchinnikov, J. Low Temp. Phys. **34**, 409 (1979).
[29] V.M. Vinokur, P.H. Kes, and A.E. Koshelev, Physica C **168**, 29 (1990).
[30] M. Niderost, A. Suter, P. Visani, A.C. Mota, and G. Blatter, Phys. Rev. B **53**, 9286 (1996).
[31] Y. Radzyner, A. Shaulov, Y. Yeshurun, I. Felner, K. Kishio, and J. Shimoyama, Phys. Rev. B **65**, 100503 (2002).
[32] M. Konczykowski, C.J. van der Beek, S. Colson, M.V. Indenbom, P.H. Kes, Y. Paltiel and E. Zeldov, Physica C **341-348**, 1317 (2000).
[33] H. Kpfer, S.N. Gordeev, W. Jahn, R. Kresse, R. Meier-Hirmer, T.

Wolf, A.A. Zhukov, K. Salama, and D. Lee, Phys. Rev. B **50**, 7016 (1994).
[34] Y. Kodama, K. Oka, Y. Yamaguchi, Y. Nishihara, and K. Kajimura, Phys. Rev. B **56**, 6265 (1997).
[35] M. Pissas, D. Stamopoulos, E. Moraitakis, G. Kallias, D. Niarchos, and M. Charalambous, Phys. Rev. B **59**, 12 121 (1999).
[36] V.B. Geshkenbein, A.I. Larkin, M.V. Feigel'man, and M.V. Vinokur, Physica C **162-164**, 239 (1989).
[37] V.M. Vinokur, A.E. Koshelev, and P.H. Kes, Physica C **248**, 179 (1995).